

OPEN ACCESS

Improving energy resolution on neutron monochromator arrays

To cite this article: Markos Skoulatos *et al* 2012 *J. Phys.: Conf. Ser.* **340** 012019

View the [article online](#) for updates and enhancements.

You may also like

- [Time- and Space-Focusing Detector System for Real-Time Electron Beam Testing](#)
Koji Nakamae and Hiromu Fujioka Ura
- [Analytical derivation of the point spread function for pinhole collimators](#)
Girish Bal and Paul D Acton
- [MACS—a new high intensity cold neutron spectrometer at NIST](#)
J A Rodriguez, D M Adler, P C Brand *et al.*

Recent citations

- [Optimizing the triple-axis spectrometer PANDA at the MLZ for small samples and complex sample environment conditions](#)
C. Utschick *et al*
- [Prismatic analyser concept for neutron spectrometers](#)
Jonas O. Birk *et al*
- [Gains from the upgrade of the cold neutron triple-axis spectrometer FLEXX at the BER-II reactor](#)
M.D. Le *et al*



The Electrochemical Society
Advancing solid state & electrochemical science & technology

241st ECS Meeting

May 29 – June 2, 2022 Vancouver • BC • Canada

Abstract submission deadline: Dec 3, 2021

Connect. Engage. Champion. Empower. Accelerate.
We move science forward



Submit your abstract



Improving energy resolution on neutron monochromator arrays

Markos Skoulatos, Klaus Habicht and Klaus Lieutenant

Helmholtz Zentrum Berlin, Berlin, 14109, Germany

markos.skoulatos@helmholtz-berlin.de

Abstract. Horizontal focusing properties of a new neutron monochromator geometry are investigated by Monte Carlo simulations. The geometry is based on the Rowland circle, which satisfies ideal focusing conditions, as opposed to standard planar monochromator devices. For asymmetric geometries one can get optimised conditions for both intensity and energy resolution for such a “Rowland monochromator”, in contrast to standard planar arrays. Energy resolution gains are also found for symmetric geometries, in particular for cold neutrons. Additional advantages include a symmetric beam well centered in energy. No changes are observed in integrated intensities.

Since many decades, neutron monochromators have been used for both diffraction and inelastic experiments in neutron reactors as well as spallation sources, in order to focus in real and k -space [1]. In particular, focusing properties have been employed exhaustively in different experimental setups by means of focusing with a planar array of crystals onto a spot (sample for a monochromator or detector for an analyser).

However, there is a further potential in using neutron monochromators which has not been exploited so far, due to its complexity in design or lack of Monte Carlo (MC) simulation results. Let us describe this arrangement, which is based on the so-called Rowland circle geometry [2] and a Johansson type curved crystal [3], most common for x-ray setups. In order to satisfy the ideal focusing condition, the source (A), monochromator (B) and sample (C) must lie on the Rowland circle, as shown in fig. 1. We stress that in this ideal case, the monochromator surface is not planar, but instead lies on the Rowland circle, with center R . Furthermore, the orientation of the lattice planes of the reflecting crystallites are determined by a different circle which we call the focusing circle, with center F . For the general asymmetric Rowland case, in which $AB \neq BC$, points B , R and F are not collinear. This introduces the angle $\delta\theta$, which equals 0 for the symmetric Rowland geometry ($AB=BC$). This general layout forms the basis of our motivation to study neutron monochromator properties, since the focusing circle is being used extensively, unlike the Rowland circle which has never been reported on neutron monochromators.

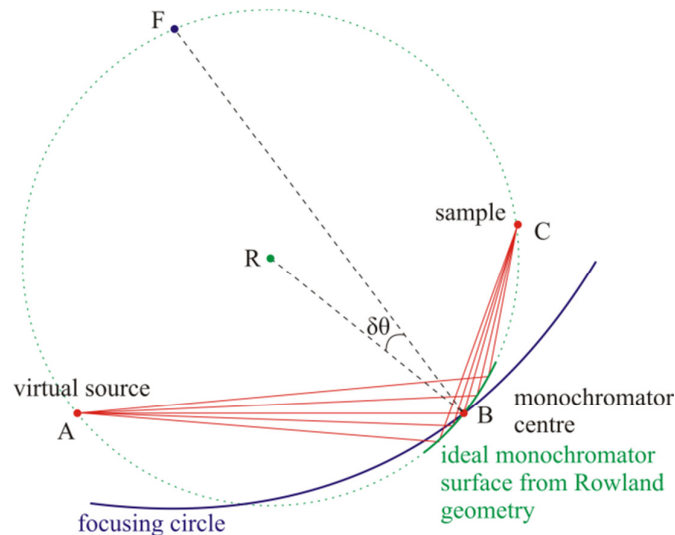


Figure 1 Rowland circle geometry indicating the Rowland and focusing circles. Distances here are $AB=2\text{m}$ and $BC=1\text{m}$.

In order to investigate this model, we construct a generic instrument within the McStas [4,5] MC simulation package, which consists of a neutron source, followed by a slit (which plays the role of a virtual source, read more on [6]), a monochromator and a monitor, as shown in fig. 2a). The distances slit-monochromator and monochromator-monitor are equal to L_1 and L_2 respectively and can be varied. For a practical application of such a neutron monochromator it is necessary to be able to change the selected wavelength (and hence the radii of curvature and Rowland circle simultaneously). We approximate the ideal case described in fig. 1, by that shown in Model B of fig. 2b), where individual crystal pieces are arranged with their centres on the Rowland circle. We compare this model to a standard planar monochromator (Model A) as well as a hybrid case (Model C). This last model is a mixture of models A and B as it is a planar device, however it is still a good approximation of the Rowland circle for the loci of the monochromator pieces. The way this is achieved is by including the extra $\delta\theta$ in the take-off angle of the whole array, while turning back every individual crystal by $-\delta\theta$ in order to satisfy the elastic condition. It is essentially a linear approximation of a small arc of the Rowland circle, and only requires individually turning each piece, however not shifting them on the exact Rowland circle as is required by model B. A similar setup to this engineering design (Model C) is in use at the MACS [7,8] monochromator and as a multiplexing analyser-detector system in various triple-axis spectrometers, including the RITA-II [9,10], SPINS [11], IMPS [12] option at IN8, SIKA [13], MACS [14], as well as PUMA [15] and UFO [16,17] option of IN12, with the last two having more degrees of freedom. Note however that, with the exception of the MACS monochromator, their usage is completely different, focusing primarily on simultaneous data collection in (Q, ω) space (multiplexing). We emphasize on the use of such a design for the monochromator (elastic case), which in addition spatially focuses onto the sample (and does not disperse on a position sensitive detector). Furthermore, the shifts we are interested in are those dictated purely by the Rowland geometry, unlike shifts of the PUMA and UFO option, which are on a kinematic basis for following particular paths in (Q, ω) .

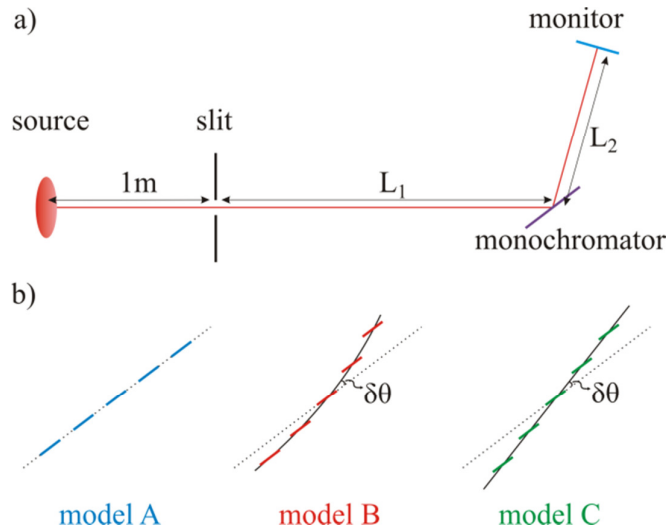


Figure 2 Monte Carlo simulation model ($L_1=2\text{m}$, $L_2=1\text{m}$ and $\lambda=4.05 \text{ \AA}$). Part a) shows the whole instrument layout, and b) the 3 different monochromator modules simulated: A: standard planar, B: Rowland, C: hybrid geometry. In the monochromator models B and C, the dashed line is taken from model A for comparison. For simplicity we only show 5 monochromator crystals which correspond to an unfocused device in this figure.

For the MC simulations we assume a 31cm array in the horizontal plane, consisting of 1cm pyrolytic graphite (PG) crystals in the (002) orientation, with mosaic $\eta=30^\circ$. Simulations were performed for both cold and thermal neutrons ($\lambda=4.05$ and 1.8 \AA), while the sample has a width of 1 cm in the horizontal plane. Three distinct cases are modelled: the symmetric Rowland geometry ($L_1=L_2$) and two asymmetric cases ($L_1>L_2$ and $L_1<L_2$). Note that optimal focusing for model A is determined analytically by the standard formula

$$R_{\text{Model A}}^{\text{standard}} = \frac{2L_1L_2}{L_1+L_2} \frac{1}{\sin\theta} \quad \text{eq. (1),}$$

whilst for models B/C the following can be shown [18]:

$$R_{\text{Models B/C}}^{\text{hor. shifts}} = \frac{L_1+L_2}{2\sin\theta} \quad \text{eq. (2).}$$

Apart from the analytical derivations, both of these equations have been also verified during these M.C. simulations. Optimum focusing is used throughout.

The results, summarized in fig. 3 are striking. In all cases, model B gives a better energy resolution (FWHM throughout) and overall beam properties (symmetry and nominal center). In particular, for the asymmetric cases the energy resolution gets drastically better (a factor of 3-8) as a result of following the right crystal geometry. We can understand this qualitatively by inspecting model B of fig. 2b. This is a drawing (in scale) of how far away the crystal elements are in standard monochromators (dashed line) compared to the ideal case (solid red lines). Note that fig. 2 is for an asymmetric case (for the symmetric one the shifts are much smaller, hence smaller gains there).

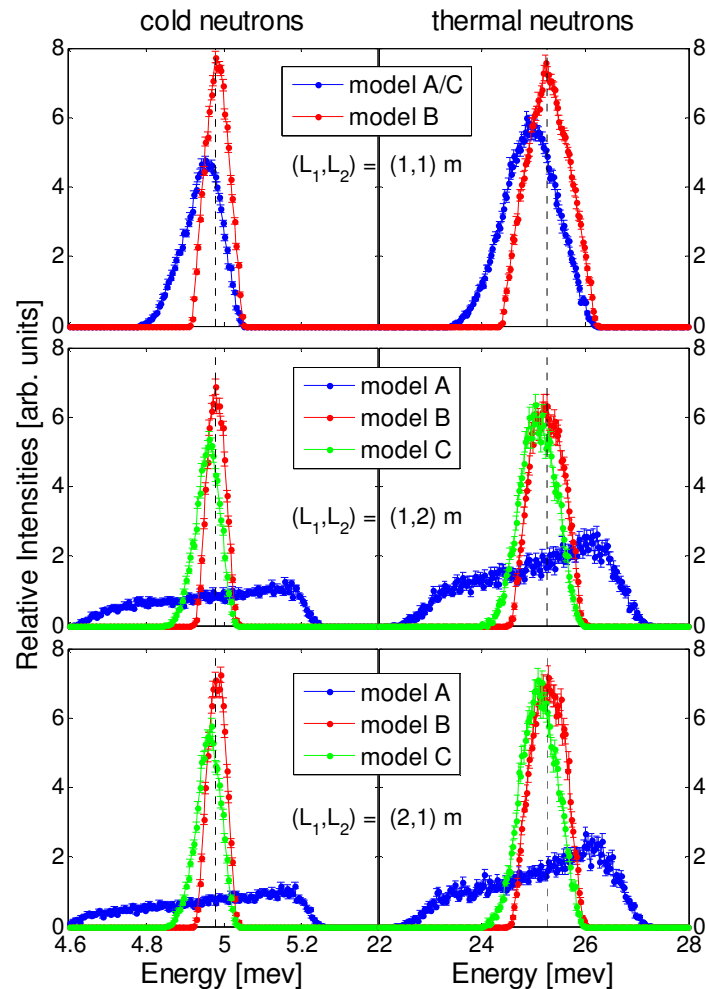


Figure 3 McStas MC simulation results for cold (left) and thermal (right) neutrons. The top part shows a symmetric geometry while the middle and bottom plots are for asymmetric cases. Large energy resolution gains are obtained by using models B/C, while in particular model B (“Rowland monochromator”) benefits on top from symmetric energy lineshapes which are well-centered w.r.t. the nominal energy.

For cold neutrons and for the symmetric Rowland geometry we get a 43% increase in energy resolution (and a 5% increase in integrated intensity) when comparing model B to A (equivalent to C). Furthermore, the energy lineshape forms a very symmetric peak and in addition is well centered to the nominal energy for the given monochromator take-off angle, indicated by the dashed line in fig. 3 (model A deviates by 25 μeV , a significant fraction of the energy resolution that can be important when studying low-gapped excited states). For $L_1=1\text{m}$, $L_2=2\text{m}$ the energy resolution gets drastically better with ratios 1:7.6:6.3 for models A:B:C respectively. Similarly for $L_1=2\text{m}$, $L_2=1\text{m}$ the energy resolution ratios are 1:7.1:6.0 for models A:B:C. In all cases, the integrated intensities are similar with small

deviations around 3-5%. This is a real effect and comes from the size of the monochromator as viewed by the source, since the whole device is tilted when changing configurations and is a side effect.

For thermal neutrons and the symmetric Rowland scenario with $L_1=L_2=1\text{m}$ we have a small gain of 13% in the energy resolution. This happens because the deviations away from the ideal Rowland geometry are smaller at these wavelengths. However, the peak is more symmetric and centered exactly at the nominal wavelength for the given take-off angle as shown in fig. 3. For the asymmetric cases we find that models B and C give similar results in width, however model B is indeed better centered. The energy resolution gains are large for thermal wavelengths too: for $L_1=1\text{m}$, $L_2=2\text{m}$ ($L_1=2\text{m}$, $L_2=1\text{m}$) we get ratios 1:3.5 (1:3.1) when comparing models A:B.

In general, when designing an instrument the distance from the real neutron source to the monochromator is not equal to the distance from monochromator to sample. Under these conditions, one cannot achieve real and k-space focusing simultaneously. The standard solution is to introduce a virtual source by means of a slit so that $L_1=L_2$. The other way around it is to use a "Rowland" monochromator, model B (or an approximation to it as used on MACS, model C).

Summarizing, we have comprehensively shown that this Rowland monochromator gives in all cases good intensity and energy resolution simultaneously. Furthermore, the beam one gets is symmetric in energy and centred at the correct energy corresponding to the nominal monochromator take-off angle. These gains in energy resolution as well as energy lineshapes are also observed for symmetric Rowland cases and are larger for the colder wavelengths. The multiplexing secondary spectrometers existing to date are a clear indication that the technology for such a device exists. What is needed on top of the horizontal shifts and focusing is to combine independent vertical focusing in order to create such beneficial instruments.

Acknowledgements MS would like to thank E. Farhi, P. Willendrup, P. Freeman and N. Tsapatsaris for useful information and discussions.

References

- [1] Proc. Workshop on Focusing Bragg Optics, Braunschweig Germany 1993 *Nucl. Instr. and Meth. A* **338**
- [2] Born M and Wolf E 2002 Principles of optics, Cambridge University Press, 7th edition
- [3] Johansson T 1933 *Zeitschrift für Physik A Hadrons and Nuclei* **82** 7 507
- [4] Lefmann K and Nielsen K 1999 *Neutron News* **10** 20
- [5] Willendrup P, Farhi E and Lefmann K 2004 *Physica B* **350** 735
- [6] Habicht K and Skoulatos M Optimization of virtual source parameters in neutron scattering instrumentation, *these proceedings*
- [7] Broholm C 1996 *Nucl. Instr. and Meth. A* **369** 169
- [8] Smee S A, Orndorff J D, Scharfstein G A, Qiu Y, Brand P C, Broholm C L and Anand D K 2002 *Appl. Phys. A* **74** S255
- [9] Lefmann K, McMorro D F, Rønnow H M, Nielsen K, Clausen K N, Lake B and Aeppli G 2000 *Physica B* **283** 343
- [10] Bahl C R H, Andersen P, Klausen S N and Lefmann K 2004 *Nucl. Instr. and Meth. B* **226** 667
- [11] Zaliznyak I A and Lee S-H 2004 "Magnetic Neutron Scattering and Recent Developments in Triple Axis Spectroscopy" in Modern Techniques for Characterizing Magnetic Materials ed. by Z. Yimei, (Kluwer)
- [12] Jiménez-Ruiz M, Hiess A, Currat R, Kulda J and Bermejo F J 2006 *Physica B* **385-386** 1086
- [13] Vorderwisch P and Wu C-M, SIKa cold TAS, http://www.ansto.gov.au/_data/assets/pdf_file/0016/37042/Sika_Fact_Sheet.pdf
- [14] Rodriguez J A, Adler D M, Brand P C, Broholm C, Cook J C, Brocker C, Hammond R, Huang Z, Hundertmark P, Lynn J W, Maliszewskyj N C, Moyer J, Orndorff J, Pierce D, Pike T D, Scharfstein G, Smee S A and Vilaseca R 2008 *Meas. Sci. Technol.* **19**

- [15] Eckold G December 2009 The multianalyzer/Multidetector Design of PUMA, *FRM II news* No **3**
- [16] Schmidt W, Rheinstädter M C, Raymond S and Ohl M 2004 *Physica B* **350** e849
- [17] Schmidt W and Ohl M 2006 *Physica B* **385** 1073
- [18] Habicht K and Skoulatos M Phase-space tailoring using the virtual source concept, *review paper to be published*